Supplemental Document

OPTICA QUANTUM

Temperature-independent almost perfect photon entanglement from quantum dots via the SUPER scheme: supplement

THOMAS K. BRACHT,[1,2,*] MORITZ CYGOREK,[3] TIM SEIDELMANN,[4] VOLLRATH MARTIN AXT,[4] AND DORIS E. REITER[2]

[1] *Institut für Festkörpertheorie, Universität Münster, 48149 Münster, Germany*
[2] *Condensed Matter Theory, Department of Physics, TU Dortmund, 44221 Dortmund, Germany*
[3] *Heriot-Watt University, Edinburgh EH14 4AS, UK*
[4] *Theoretische Physik III, Universität Bayreuth, 95440 Bayreuth, Germany*
[*] *t.bracht@wwu.de*

Supplement DOI: https://doi.org/10.6084/m9.figshare.24658824

Parent Article DOI: https://doi.org/10.1364/OPTICAQ.498559

Temperature-independent almost perfect photon entanglement from quantum dots via the SUPER scheme: supplemental document

1. SYSTEM HAMILTONIAN

The quantum dot is modeled as a four-level system, which is placed inside a cavity with two cavity modes, one for each of the two orthogonal linear polarizations, X and Y. The Hamiltonian of this system reads [1, 2]

$$\begin{aligned} H_0 =& \hbar\omega_x(|X\rangle\langle X| + |Y\rangle\langle Y|) + (2\hbar\omega_x - \Delta_B)|B\rangle\langle B| \\ &+ (\hbar\omega_x - \Delta_B/2)(a_X^\dagger a_X + a_Y^\dagger a_Y), \end{aligned} \tag{S1}$$

where $\hbar\omega_x$ is the energy of the exciton states, Δ_B the biexciton binding energy (BBE) and the operators $a_{X/Y}(a_{X/Y}^\dagger)$ destroy (create) a photon in the respective cavity mode. The quantum dot is excited via an external laser and coupled to the cavity, so the electron-light interaction is given by

$$\begin{aligned} H_{\text{el}} =& -\frac{\hbar}{2}(\Omega_X(t)\sigma_X^\dagger + \Omega_Y(t)\sigma_Y^\dagger) \\ &+ \hbar g\,(a_X\sigma_X^\dagger + a_Y\sigma_Y^\dagger) + \text{h.c.}. \end{aligned} \tag{S2}$$

Here, g governs the strength of coupling to the cavity, and the terms $\Omega_{X/Y}(t)$ describe the field of the laser used to excite the quantum dot with the respective linear polarization operators $\sigma_S = |G\rangle\langle S| + |S\rangle\langle B|$, where $S \in \{X, Y\}$.
For the production of photon entanglement, the cavity used is resonant with the two-photon transition. This offers the advantage that the QD only has to be tuned to match this specific transition. This is simpler compared to alternative approaches of, for example, tuning each transition (namely, $B - X/Y$ and $X/Y - G$) to correspond with individual cavity modes. Furthermore, studies have demonstrated that the scenario using a two-photon resonant cavity yields higher entanglement compared to setups where cavity modes match single transitions [3, 4]. However, it should be noted that in this setup, photon separation cannot be achieved spectrally. Instead, tools such as a beam splitter are required.
For the excitation, we assume a Gaussian-shaped pulse given by

$$\Omega(t) = \frac{\alpha}{\sqrt{2\pi\sigma^2}} e^{-\frac{t^2}{2\sigma^2}} e^{-i\omega_L t}, \tag{S3}$$

where α is the pulse area, σ is a measure of the pulse duration, which is related to the full-width at half maximum (FWHM) of the intensity by $\tau_{\text{FWHM}} = 2\sqrt{\ln(2)}\,\sigma$. The frequency of the laser pulse, denoted by ω_L, is connected to the detuning to the quantum dot ground-state to exciton transition by $\Delta = \hbar(\omega_L - \omega_x)$.

The state preparation in quantum dots is disturbed by the surrounding environment. At low temperatures, the influence of longitudinal acoustic phonons acts as a limiting effect, this interaction with the lattice vibrations is modeled using the pure-dephasing type Hamiltonian

$$\begin{aligned} H_{\text{ph}} =& \hbar\sum_{\mathbf{q}} \omega_{\mathbf{q}} b_{\mathbf{q}}^\dagger b_{\mathbf{q}} + \hbar(|X\rangle\langle X| + |Y\rangle\langle Y| + \\ & 2|B\rangle\langle B|)\sum_{\mathbf{q}} \left(g_{\mathbf{q}} b_{\mathbf{q}} + g_{\mathbf{q}}^* b_{\mathbf{q}}^\dagger\right). \end{aligned} \tag{S4}$$

Table S1. Parameters that are used in the simulations, unless mentioned otherwise.

Parameter	Symbol	Value
Fine-structure splitting	$\hbar\delta_0$	0 meV
Biexciton binding energy	Δ_B	1 meV
Radiative decay rate, X/Y	γ_x	0.01 ps^{-1}
Radiative decay rate, B	$\gamma_B = 2\gamma_x$	0.02 ps^{-1}
Cavity coupling	$\hbar g$	0.06 meV
Cavity outcoupling	$\hbar\kappa$	0.12 meV
Detuning, pulse 1	Δ_1	-5 meV
Detuning, pulse 2	Δ_2	-12.96 meV
Pulse area, pulse 1	α_1	32π
Pulse area, pulse 2	α_2	12.8π
Pulse durations	$\sigma_{1/2}$	2.7 ps

The operator $b^\dagger_{\mathbf{q}}(b_{\mathbf{q}})$ creates (destroys) a phonon with wave vector $\mathbf{q}$. The phonons are coupled to the exciton states with the coupling element $g_{\mathbf{q}}$ and follow the linear dispersion relation $\omega_{\mathbf{q}} = c_{\mathrm{LA}}q$, where c_{LA} is the velocity of sound in the material. Containing two excitons, the coupling to the biexciton is twice as strong. We use the same material parameters as in Ref. [5], with an electron confinement length (size of the quantum dot) of 5 nm.

The photons emitted by the quantum dot are modeled using Lindblad operators $\mathcal{L}$,

$$\mathcal{L}_{O,\gamma}\rho = \frac{\gamma}{2}\left(2O\rho O^\dagger - O^\dagger O\rho - \rho O^\dagger O\right). \tag{S5}$$

For the radiative decay with rate γ, this leads to the Operators $\mathcal{L}_{|G\rangle\langle X|,\gamma_x}$, $\mathcal{L}_{|G\rangle\langle Y|,\gamma_x}$, $\mathcal{L}_{|X\rangle\langle B|,\gamma_B/2}$, $\mathcal{L}_{|Y\rangle\langle B|,\gamma_B/2}$. The out-coupling of photons from the cavity with rate κ leads to the operators $\mathcal{L}_{a_X,\kappa}$, $\mathcal{L}_{a_Y,\kappa}$. The parameters used in the calculations are given in Tab. S1.

2. CALCULATION OF THE CONCURRENCE

To quantify the degree of entanglement, we utilize the concurrence as a measure of the entanglement degree [6]. The concurrence is determined from the two-photon density matrix ρ^{2P} by evaluating the four eigenvalues λ_i of the matrix

$$M = \rho^{\mathrm{2P}} T \rho^{\mathrm{2P}^*} T, \tag{S6}$$

where ρ^{2P^*} represents the complex conjugate of the two-photon density matrix and T is the anti-diagonal matrix with the elements $(-1, 1, 1, -1)$. After sorting the eigenvalues in decreasing order, i.e., $\lambda_{i+1} \leq \lambda_i$, the concurrence is then given by [6, 7]

$$C = \max\left\{0, \sqrt{\lambda_1} - \sqrt{\lambda_2} - \sqrt{\lambda_3} - \sqrt{\lambda_4}\right\}. \tag{S7}$$

The two-photon density matrix ρ^{2P} is calculated using two-time correlation functions of the transition operators $\tilde{\sigma}_{X/Y}$, as explained in detail in Ref. [8] (SI). In calculations without a cavity, the transition operators correspond to the polarization operators, i.e., $\tilde{\sigma}_{X/Y} = \sigma_{X/Y}$. In calculations including a cavity, the transition operators correspond to the cavity photon operators, i.e., $\tilde{\sigma}_{X/Y} = a_{X/Y}$. These operators are then used in the two-time correlation functions of the form

$$G^{(2)}_{AB,CD}(t,\tau) = \langle \tilde{\sigma}^\dagger_A(t)\tilde{\sigma}^\dagger_B(t+\tau)\tilde{\sigma}_D(t+\tau)\tilde{\sigma}_C(t)\rangle. \tag{S8}$$

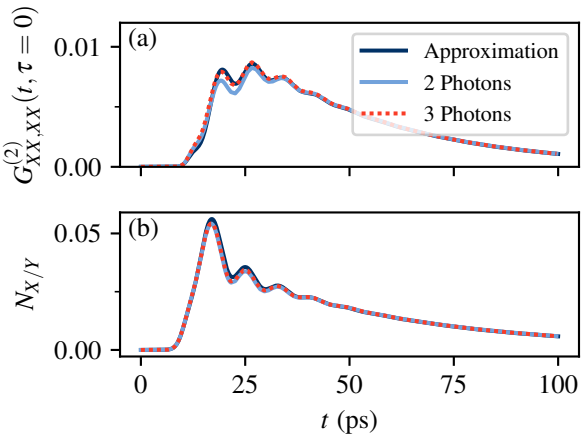

Fig. S1. (a) Exemplary $G^{(2)}_{XX,XX}(t,\tau=0)$ for TPE, and (b) the dynamics of the cavity photon number $N_{X/Y}$ for calculations including two and three photons per cavity mode, compared to the approximation including one photon per cavity mode and the states $|G,2,0\rangle$ and $|G,0,2\rangle$.

Due to numerical limitations, calculations including phonons and the cavity consider only one photon per X/Y polarized cavity mode. In addition, the states consisting of the quantum dot's ground state and two photons per cavity mode (i.e., $|G,n_X=2,n_Y=0\rangle$, $|G,n_X=0,n_Y=2\rangle$) are included to ensure accurate results in the two-time correlation functions. Specifically, the correlation functions of the type $G^{(2)}_{XX,XX}(t,\tau=0)=\langle a^\dagger_X(t)a^\dagger_X(t)a_X(t)a_X(t)\rangle$ would always be zero if only one photon per cavity mode was considered.
By using this approach, the Hilbert space dimension is reduced to 18 $(=4\times2\times2+2)$ instead of 36 if two photons were fully included. This approximation significantly reduces the computation time, as the numerical effort including phonons scales unfavorably with the dimension. We have verified in the phonon-free case, comparing calculations made with the approximation and the complete inclusion of two and three photons per cavity mode, that including more photons has only negligible effects on the population dynamics and concurrence values for the parameter regime studied in this paper.
Figure S1 illustrates the impact of the approximation for the case of TPE (same parameters as in Fig. 3) without phonons. Panel (a) displays the two-time correlation $G^{(2)}_{XX,XX}(t,\tau=0)$, revealing only minor deviations around $t\sim20\,$ps, when compared to calculations that fully include two or three photons per cavity mode. Similarly, panel (b) presents the dynamics of the cavity photon number, also demonstrating only slight deviations.

3. NUMERICAL OPTIMIZATION FOR SUPER PARAMETERS

In Fig 2 in the main document, it was observed that a high concurrence exceeding $C=99\,\%$ could be achieved over a wide range of parameters. Here, the excitation parameters for each set were found through numerical optimization of the final biexciton occupation. Due to the computational complexity involved in calculating the concurrence values, the parameters for the SUPER scheme were optimized based on the biexciton population rather than directly optimizing the concurrence. This approach is valuable in the way that it automatically provides results where a high photon rate can be expected. For each values of α_1 and Δ_B, with a fixed $\Delta_1=-5\,$meV, the optimal α_2,Δ_2 were determined. The pulse areas $\alpha_{1/2}$ were constrained to a maximum value of 35π.

Figure S2 shows the final occupation of the biexciton state using the same parameters as in Fig 2. It is evident that for small pulse areas α_1, the preparation fidelity drops rapidly. This outcome is expected, as previous studies demonstrated that a high pulse area has to be used for the scheme to work as intended [9, 10]. Interestingly, for intermediate biexciton binding energies (BBEs), the preparation fidelity decreased to $70\,\%-80\,\%$. Due to the complex swing-up mechanism, there is no simple, straightforward explanation for this decrease in this parameter regime.
We attribute it to the different system energies for varying BBEs that influence the mixing of

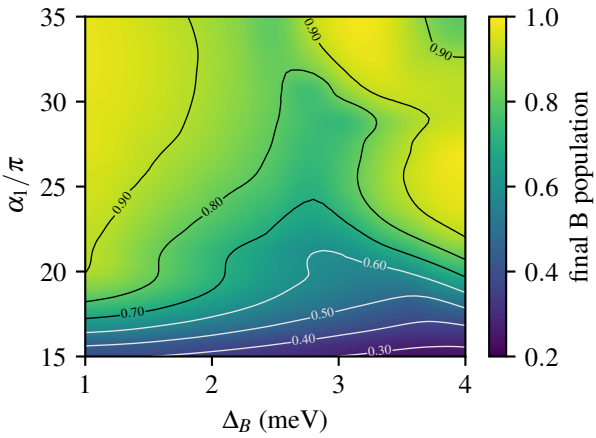

Fig. S2. The final biexciton populations (disregarding decay, cavity coupling and phonons) for the same parameters as in Fig. 2 in the main document: The parameters of the second pulse are optimized for a maximum final biexciton population.

the dressed states, leading to a more or less optimal preparation depending on the interplay of the dressed states as shown in Ref. [10]. This finding highlights that the regimes for optimal concurrence and preparation fidelity (which, in turn, effects the photon rate) may differ. In the presented case, both reach high values for small biexciton bindings and high α_1. The parameter set that yields the highest population, here for $\alpha_1 = 32\pi$, was then chosen for the further investigations.

4. IMPACT OF CAVITY COUPLING

In all previous calculations involving a cavity, a constant cavity coupling strength of $\hbar g = 0.06\,\text{meV}$ was used alongside a constant cavity out-coupling rate of $\hbar\kappa = 0.12\,\text{meV}$.
Figure S3 illustrates the influence of the cavity coupling on the concurrence and the number of photon pairs emitted via the cavity for (a) SUPER and (b) TPE. For SUPER, a plateau-like region emerges for cavity couplings up to approximately $\hbar g \sim 0.2\,\text{meV}$, beyond which the concurrence gradually decreases. The number of emitted photon pairs with the same polarization ($N^P_{XX/YY}$) rises sharply, as for small cavity couplings, the photons are emitted free-space before coupling to the cavity. With a smaller γ, i.e., a longer lifetime, as typically found in most quantum dots [11, 12], an even greater share of photon pairs is emitted via the cavity, so that an arbitrarily high concurrence and a high photon yield can be achieved simultaneously.

As the cavity coupling strength increases, a larger portion of the emitted photons pass through the cavity. Eventually, almost the entire excitation of the quantum dot is transferred to cavity photon pairs. For very large couplings $\hbar g > 0.75\,\text{meV}$, additional photons are created due to re-excitation during the laser pulse.
The number of photon pairs with different polarizations ($N^P_{XY/YX}$) detrimental to the concurrence rises only slowly with increasing coupling values. This behavior can be largely contributed to the decoupling of the cavity from the QD during the preparation process. When the biexciton is prepared and no emission occurs during the pulses, photons are only emitted to the $|XX\rangle$ and $|YY\rangle$ states. A higher coupling efficiency increases the probability of photons being emitted already during the pulse.

In contrast, for TPE in a cavity, the absence of the decoupling mechanism results in a strong impact of the enhanced photon emission on the concurrence, as depicted in Fig. S3(b). Immediately, detrimental photon pairs are created during the preparation process, causing the concurrence to rapidly drop to zero. With increasing cavity couplings exceeding $\hbar g \sim 0.3\,\text{meV}$, the number of emitted photon pairs also decreases, as the strong energy shift resulting from the dot-cavity coupling hinders efficient population transfer.

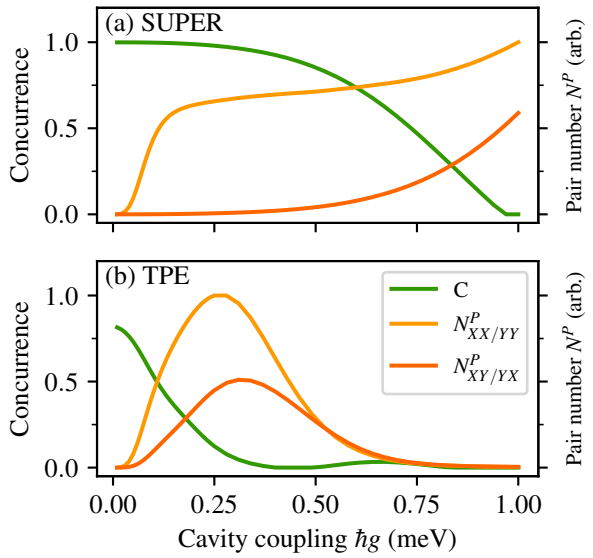

Fig. S3. (a) Concurrence and the number of photon pairs emitted via the cavity for SUPER-excitation with the same parameters as in Fig. 3 in the main document, depending on the dot-cavity coupling g. It is visible that for a strong dot-cavity coupling, the concurrence drops to zero. In this regime, the decay is strongly enhanced such that the quantum dot already emits the photons during the state preparation process, leading to photon pairs in the detrimental $|XY\rangle$ and $|YX\rangle$ state. (b) same for TPE, where due to the lack of the decoupling, the creation of detrimental photon pairs sets in immediately.

5. INFLUENCE OF TEMPERATURE ON POPULATION DYNAMICS

In Figure 4 in the main document, it was visible that the influence of the temperature shows significant differences between SUPER and TPE. Up to 77 K, the final biexciton population only slightly decreases for SUPER, when compared to TPE. Involving a cavity, the concurrence basically remains a constant 99 % for SUPER, while it starts at about 69 % for TPE at $T = 4$ K and decreases with rising temperature.

The findings for TPE are in agreement with previous studies [1, 13] that identified phonons as being a substantial source of decoherence, leading to a decrease of the concurrence. Phonons lead to renormalization of the cavity-dot coupling, effectively weakening the interaction [13].

The impact of phonons to the photon output can be seen in the population dynamics shown in Fig. S4. Panel (c) displays the number of X/Y photons in the cavity, revealing that, when phonons are included, fewer photons are emitted into the cavity at early times compared to the phonon-free case. Additionally, the oscillations are damped. Panel (a) and (b) show the population dynamics of the dot states for SUPER and TPE, respectively, indicating that phonons disturb the process of TPE substantially more than SUPER.

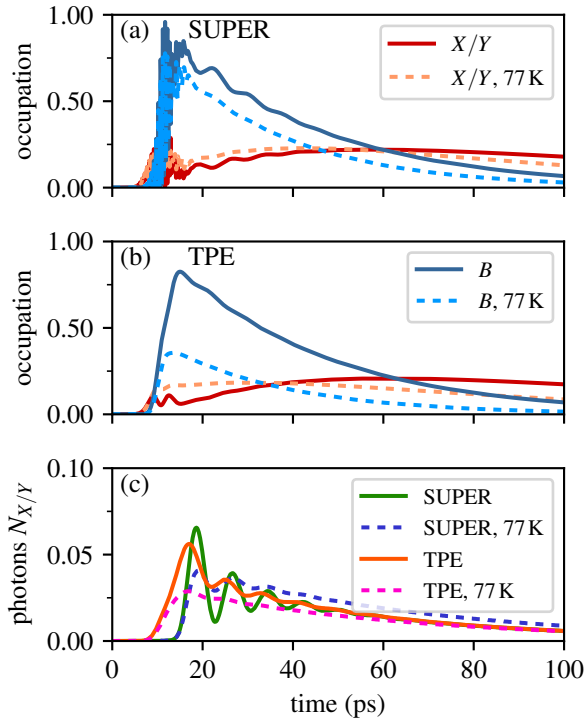

Fig. S4. The influence of longitudinal acoustic phonons on the dynamics of (a) SUPER and (b) TPE in a cavity. The number of photons in the cavity is shown in (c).

REFERENCES

1. D. Heinze, A. Zrenner, and S. Schumacher, "Polarization-entangled twin photons from two-photon quantum-dot emission," Phys. Rev. B **95**, 245306 (2017).
2. M. Cygorek, F. Ungar, T. Seidelmann, A. M. Barth, A. Vagov, V. M. Axt, and T. Kuhn, "Comparison of different concurrences characterizing photon pairs generated in the biexciton cascade in quantum dots coupled to microcavities," Phys. Rev. B **98**, 045303 (2018).
3. E. del Valle, "Distilling one, two and entangled pairs of photons from a quantum dot with cavity qed effects and spectral filtering," New J. Phys. **15**, 025019 (2013).
4. T. Seidelmann, F. Ungar, M. Cygorek, A. Vagov, A. M. Barth, T. Kuhn, and V. M. Axt, "From strong to weak temperature dependence of the two-photon entanglement resulting from the biexciton cascade inside a cavity," Phys. Rev. B **99**, 245301 (2019).
5. T. K. Bracht, T. Seidelmann, T. Kuhn, V. M. Axt, and D. E. Reiter, "Phonon wave packet emission during state preparation of a semiconductor quantum dot using different schemes," phys. status solidi (b) **259**, 2100649 (2022).
6. W. K. Wootters, "Entanglement of formation of an arbitrary state of two qubits," Phys. Rev. Lett. **80**, 2245–2248 (1998).
7. D. F. V. James, P. G. Kwiat, W. J. Munro, and A. G. White, "Measurement of qubits," Phys. Rev. A **64**, 052312 (2001).
8. T. Seidelmann, C. Schimpf, T. K. Bracht, M. Cosacchi, A. Vagov, A. Rastelli, D. E. Reiter, and V. M. Axt, "Two-photon excitation sets limit to entangled photon pair generation from quantum emitters," Phys. Rev. Lett. **129**, 193604 (2022).
9. T. K. Bracht, M. Cosacchi, T. Seidelmann, M. Cygorek, A. Vagov, V. M. Axt, T. Heindel, and D. E. Reiter, "Swing-up of quantum emitter population using detuned pulses," PRX Quantum **2**, 040354 (2021).
10. T. K. Bracht, T. Seidelmann, Y. Karli, F. Kappe, V. Remesh, G. Weihs, V. M. Axt, and D. E. Reiter, "Dressed-state analysis of two-color excitation schemes," Phys. Rev. B **107**, 035425 (2023).
11. C. Schimpf, M. Reindl, F. Basso Basset, K. D. Jöns, R. Trotta, and A. Rastelli, "Quantum

dots as potential sources of strongly entangled photons: Perspectives and challenges for applications in quantum networks," Appl. Phys. Lett. **118**, 100502 (2021).
12. L. Hanschke, K. A. Fischer, S. Appel, D. Lukin, J. Wierzbowski, S. Sun, R. Trivedi, J. Vučković, J. J. Finley, and K. Müller, "Quantum dot single-photon sources with ultra-low multi-photon probability," npj Quantum Inf. **4**, 43 (2018).
13. T. Seidelmann, F. Ungar, A. M. Barth, A. Vagov, V. M. Axt, M. Cygorek, and T. Kuhn, "Phonon-induced enhancement of photon entanglement in quantum dot-cavity systems," Phys. Rev. Lett. **123**, 137401 (2019).